Journal Name

ARTICLE

Combined PDF and Rietveld studies of ADORable zeolites and the disordered intermediate IPC-1P

Received 00th January 20xx,
Accepted 00th January 20xx

DOI: 10.1039/x0xx00000x

www.rsc.org/

Samuel A. Morris,[a] Paul S. Wheatley,[a] Miroslav Položij,[b] Petr Nachtigall,[b] Pavla Eliášová,[b] Jiří Čejka,[c] Tim C. Lucas,[d] Joseph A. Hriljac,[d] Ana B. Pinar[e] and Russell E. Morris*[a]

The disordered intermediate of the ADORable zeolite UTL has been structurally confirmed using the pair distribution function (PDF) technique. The intermediate, IPC-1P, is a disordered layered compound formed by the hydrolysis of UTL in 0.1M hydrochloric acid solution. Its structure is unsolveable by traditional X-ray diffraction techniques. The PDF technique was first benchmarked against high-quality synchrotron Rietveld refinements of IPC-2 (OKO) and IPC-4 (PCR) – two end products of IPC-1P condensation that share very similar structural features. An IPC-1P starting model derived from density functional theory was used for the PDF refinement, which yielded a final fit of *Rw* = 18% and a geometrically reasonable structure. This confirms the layers do stay intact throughout the ADOR process and shows PDF is a viable technique for layered zeolite structure determination.

Introduction

Traditionally, zeolites have been studied in their three-dimensional form; recently however, layered two-dimensional zeolites have been increasingly studied for their interesting physical properties and catalytic benefits.[1,2] Unlike their three-dimensional counterparts, chemical manipulation of two-dimensional zeolites by intercalation,[3] swelling,[4] delamination[5] and pillaring[6] leads to structural and functional versatility. An excellent review of layered zeolites by Diaz and Corma describes, in detail, the recent developments and intricacies of the field.[7, 8]

The *A*ssembly *D*isassembly *O*rganisation *R*eassembly (ADOR) process controllably breaks apart pre-assembled three-dimensional zeolites, specifically UTL,[9, 10] IWR[11] and IWW,[12] into two-dimensional layers by exploiting chemical weakness intrinsic to the parent zeolite.[13, 14] The layered building units can then be organised into suitable orientations such that condensation via calcination yields predictable, new, three-dimensional zeolites, some of which were previously designated as being unrealistic synthesis targets.[15]

For UTL, disassembly occurs by removing the Ge-rich double-four rings (D4Rs) that separate the layers by hydrolysis using dilute hydrochloric acid. The silica-rich lamellar product, IPC-1P, can be reorganised in a variety of ways and assembled through calcination into novel zeolites IPC-2 (OKO), IPC-4 (PCR), IPC-6, IPC-9 and IPC-10.[16-18] IPC-2 and IPC-4 share the same layers, but their interlayer connectivities differ. IPC-2 has a single-four ring (S4R) layer connector forming intersecting 10- and 12- ring channels, whilst IPC-4 has an oxygen atom connecting the layers, which yields smaller 8- and 10- ring channels.

IPC-1P has been previously characterised by powder X-ray diffraction (PXRD), transmission electron microscopy (TEM), theoretical simulations, chemical analysis, Fourier transform infra-red (FTIR) spectroscopy and porosity measurements.[10, 19] PXRD shows that hydrolysis causes the abundance of diffraction lines shown by UTL to reduce into a single dominant reflection and several low intensity peaks. The former corresponds to the interlayer separation and has a d-spacing of 1.2 ± 0.1 nm. All other peaks arise from 0kl intralayer reflections that are relatively invariant to subsequent treatments, such as swelling, intercalation and calcination — indicating that the UTL layers remain intact. FTIR and TEM images support this theory;[10, 19] FTIR skeletal vibrations change little between treatments and TEM images, collected perpendicular to the layer stacking, depict a layer separation of ~ 1.1 nm.

The disordered lamellar structure of IPC-1P is difficult to determine by single-crystal and powder XRD as they only probe the average, crystalline structure. Atomic pair distribution function analysis (PDF) has recently presented

[a] *EastChem School of Chemistry, University of St Andrews, St Andrews, Fife, Scotland, KY16 9ST. sam28@st-andrews.ac.uk*
[b] *Charles University in Prague, Faculty of Science, Department of Physical and Macromolecular Chemistry, Hlavova 2030/8, 128 43 Prague 2*
[c] *J. Heyrovský Institute of Physical Chemistry, Academy of Sciences of the Czech Republic, Department of Catalysis*
[d] *School of Chemistry, University of Birmingham, Edgbaston, Birmingham, B15 2TT, UK*
[e] *Laboratory of Crystallography, ETH Zurich, CH-8093 Zurich, Switzerland. Current affiliation: Laboratory of Catalysis and Sustainable Chemistry, Paul Scherrer Institute, CH-5232 Villigen, Switzerland*
Electronic Supplementary Information (ESI) available: [details of any supplementary information available should be included here]. See DOI: 10.1039/x0xx00000x

itself as a viable option for local structure determination of highly faulted materials, by providing experimental data against which a model can be refined, akin to the Rietveld analysis for PXRD.[20, 21] This type of refinement has been used to great effect when studying the mechanism of a single-crystal to disordered to single-crystal phase transition that occurs in the MOF Cu-SIP-3.[22] PDF has also been to study battery processes, providing interesting structural information as the battery charges and discharges.[23-25] The pair distribution function is a histogram of atomic spacing between pairs of atoms in the material. An advantage of the PDF technique is that it contains information from both the long-range and local non-periodic or disordered atomic structure by treating Bragg and diffuse scattering events equally. The PDF, *G(r)*, is a real-space function and is interpretable without an initial model; each peak in the function represents the separation of pairs of atoms (See Figure 1). However, a worry with PDF is the paucity of data (at least compared with X-ray diffraction from highly crystalline materials) – will refinement against PDF data give structures of suitable quality to make strong conclusions about the structure.

To answer this latter point this paper present the PDF-derived refined structures of IPC-2 and IPC-4, which are benchmarked against Rietveld refinements of from high-quality synchrotron X-ray diffraction data. We then present the structural determination of IPC-1P using the PDF technique alone, as for this more disordered material X-ray diffraction is unsuitable.

Results

IPC-2, IPC-4 and IPC-1P all share similar primary and secondary building units (Si or Ge tetrahedra and pentasil structures respectively) and thus share similar experimental PDF patterns at interatomic distances less than 5.5 Å (Fig.1).

The peaks at 1.61, 2.62 and 3.06 Å correspond to T-O, O-O and T-T distances respectively, where T is Si, Ge or B. Peaks are weighted by bond frequency, multiplicity and by atomic scattering of the constituents, which for X-rays equates to the atomic form factor. Hence, a PDF is less sensitive to oxygen than silicon and germanium, shown here by the decreased amplitude of the O-O peak compared with the T-T peak. Peaks seen above 3.38 Å are difficult to assign to individual interatomic distances due to the overlap of contributions from multiple pairs of atoms.

Comparing the *G(r)* of IPC-2 with that of IPC-4 clearly demonstrates that this sample of IPC-2 is not as crystalline as IPC-4, whose peaks are sharper at high *r* ranges (>15 Å). This is due to the acidic conditions and extra silicon source required to produce IPC-2; $Si(CH_3)_2(OCH_2CH_2)_2$ must undergo acid catalysed condensation (in 1M HNO_3) with the correct silanol groups of IPC-1P to fully connect the layers. When compared to the simple reorganisation and condensation of IPC-1P layers required to produce IPC-4, then it is clear one process is more taxing on the framework and liable to disorder. However, it is still crystalline enough for a successful Rietveld refinement against synchrotron data. It is likely a technique like PDF will be of greatest use for samples that are of less than optimum crystallinity.

A Rietveld refinement using the GSAS program suite[10] for IPC-2 was carried out against the experimental synchrotron X-ray diffraction data, using a DFT optimised cell and atomic coordinates as a starting model. Bond angle and distance

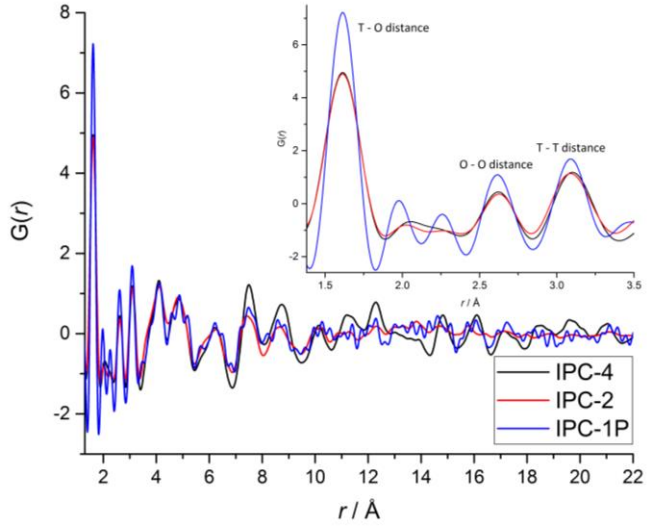

Figure 1: Experimental PDF data of IPC-4 (black line), IPC-2 (red line) and IPC-1P (blue line). The inset labels the structural features immediately discernable without modelling.

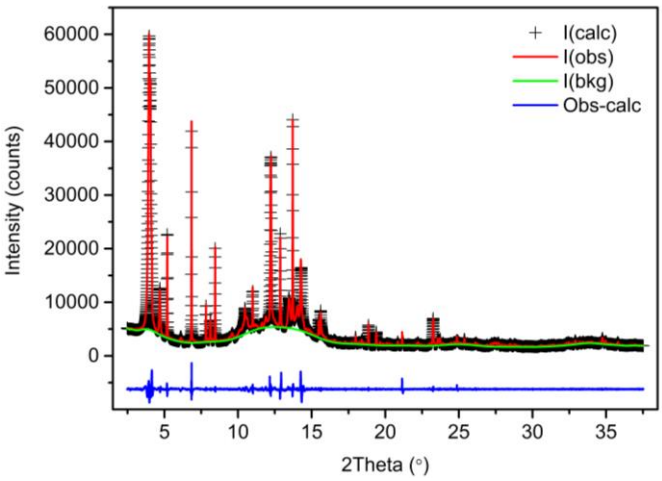

Figure 2: GSAS Rietveld refinement of IPC-2 showing the experimental synchrotron data (red), fitted calculated background (green), calculated model (+) and the observed - calculated difference curve (blue).

restraints were applied (initial weighting factor of 50 in GSAS). The structural model refinement then converged satisfactory and the restraint weighting factor was reduced slowly. The isotropic displacement factors (U_{iso}) were constrained to be equal for each atom type and refined to sensible values. The

Rietveld analysis of IPC-2 obtained a fit of R_{wp} = 0.0406 and R_F^2 = 15.82 (Fig.2).

The IPC-2 PDF refinement yielded a superb fit, with R_w = 14.89% across a 1.3 - 22 $Å^{-1}$ fit range (Fig.3). A comparison of structural parameters from the various analyses can be seen in Table 1. A comparison of bond distances, bond angles and unit cell parameters for PDF and Rietveld refinements are shown in Tables 1 to 4. These values are compared with those derived from distance least squares refinements for idealised pure silica materials taken from the International Zeolite Association website (iza-online.org). The PDF refinement produces an average Si-O bond length of 1.62 Å, only 3.3% different, on a bond-for-bond basis, from the Rietveld refinement and idealised structures but well within an acceptable range. Figure 4 shows a visual comparison of the PDF and Rietveld model structures overlaid. The largest deviations of the PDF model from the other structures occur in the S4Rs and their connection to the layers; where the PDF refined structure deviates significantly from the theoretical bond angles (O-T-O = 94.5 – 123.6 °), indicating a large amount of strain or disorder within those regions that Rietveld does not capture. This could be related to the known susceptibility of the OKO framework to form defects in this region of the structure.[26]

The main discrepancy between the PDF and Rietveld derived IPC-2 structures is the *a*-axis of the unit cell; values of 23.78 Å, 25.02 Å and 24.06 Å are calculated from the PDF refinement, Rietveld refinement and compared to the value in the IZA structure database, respectively (Table 2). Different samples were used for each refinement, meaning different levels of germanium and boron present would alter the unit cell values. All other unit cell parameters are consistent between techniques, showing the ability of PDF refinement to deal with complex systems. There is also the possibility of negative thermal expansion in zeolites[27, 28] as the data were collected at different temperatures, although further work will be needed to confirm this.

For IPC-4 (PCR), a Rietveld refinement using the program TOPAS[29] was carried out against experimental X-ray diffraction data, collected at the Material Science beam line at the Swiss Light Source, using the coordinates of an idealised structure optimised using a distance-least-squares procedure as the starting model. Geometric bond angle and distance restraints were applied and yielded a reasonable geometry for the framework. Final *R* values R_F = 0.069 and R_{wp} = 0.204 (R_{exp} = 0.066) were obtained, the crystallographic data are given in the Supplementary information (Fig.5).

The fit to the IPC-4 *G(r)* is also excellent across the 1.3 - 22 $Å^{-1}$ range with an R_w = 12.5% (Fig. 6). The PDF calculated model slightly over-estimates the initial T-O and O-O peak heights, while all other peaks are accounted for and fit well. A comparison of structural parameters with the Rietveld derived model and idealised values of Si-O bond lengths and angles can be seen in Table 3.

The PDF refined Si-O bond length average is 1.63 Å and deviates by a bond-for-bond average of 4.30% and 4.23% from the Rietveld calculated and idealised structures, respectively. The Si-O bond length range of 1.49 - 1.75 Å within the PDF calculated structure is large; the original UTL sample used contained both boron (B-O = 1.47 Å) and germanium (Ge-O = 1.73 Å) that may still be present in low concentrations, accounting for the observed range. A similar but smaller range (1.52 – 1.72 Å) was calculated for IPC-2, which can be accounted for by the same reason. The average PDF refined,

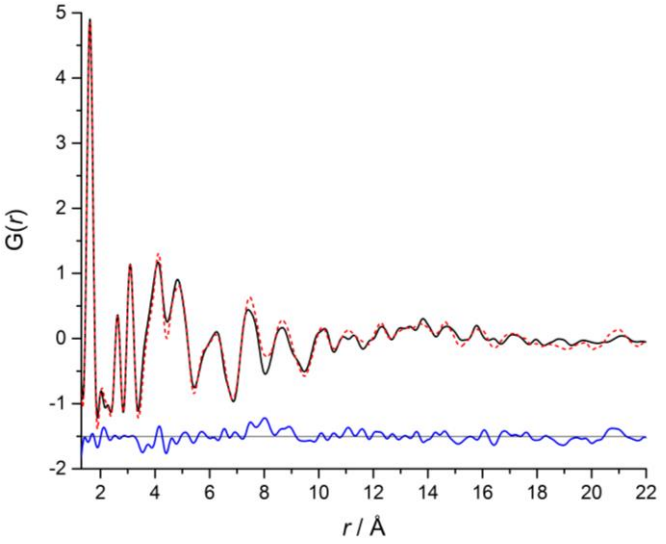

Figure 3: Refinement of the IPC-2 model against PDF data. Rw = 14.5 %. The black solid line is experimental data, the red dashed line is the calculated PDF from the model and the blue line is the difference between the two, offset by -1.5.

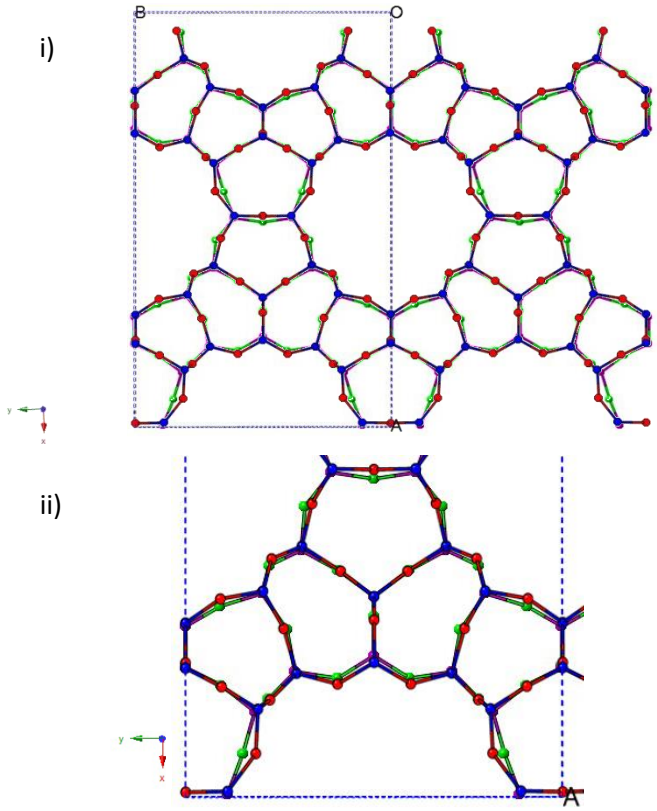

Figure 4: An overlap of IPC-2 (OKO) refinements by PDF (Si atoms in blue, O atoms in red) over Rietveld (Si atoms in purple, O atoms in green) showing the minimal differences between them. i) Shows two unit cells whilst ii) shows a zoomed in section to highlight the finer differences. The unit cells have been rescaled to allow comparison and viewed down the c-axis.

Table 1: Structural parameters for IPC-2 (OKO) calculated by different methods.

	Average Si-O Bond length / Å	Average Si-O-Si Angle / °	Average O-Si-O Angle / °
PDF Refinement	1.62	148.6	109.2
Rietveld Refinement	1.63	148.5	109.4
IZA OKO	1.61	150.1	109.5

Table 2: A structural comparison of the C2/m IPC-2 OKO structure, calculated by different methods and compared to the values in the IZA structural database.

Unit Cell	IZA OKO	PDF refinement	Rietveld refinement
a / Å	24.06	23.78	25.0184(13)
b / Å	13.83	14.08	13.82672(8)
c / Å	12.35	12.40	12.2943(12)
α / °	90	90	90
β / °	109.1	109.1	108.7179(28)
γ / °	90	90	90

Table 3: A structural parameter comparison for the IPC-4 (PCR) structure, calculated by different methods.

	Average Si-O Bond length / Å	Average Si-O-Si Angle / °	Average O-Si-O Angle / °
PDF Refinement	1.62	150.5	109.1
Rietveld Refinement	1.60	154.0	109.5
IZA PCR	1.61	154.3	109.5

Table 4: A structural comparison of parameters calculated by different methods for the IPC-4 (PCR) structure. All structures are in the spacegroup C2/m.

Unit Cell	IZA PCR	PDF Refinement	Rietveld Refinement
a / Å	20.14	20.07	20.0120(1)
b / Å	14.07	14.02	13.9193(1)
c / Å	12.52	12.44	12.30(7)
α / °	90	90	90
β / °	115.7	115.7	114.8(7)
γ / °	90	90	90

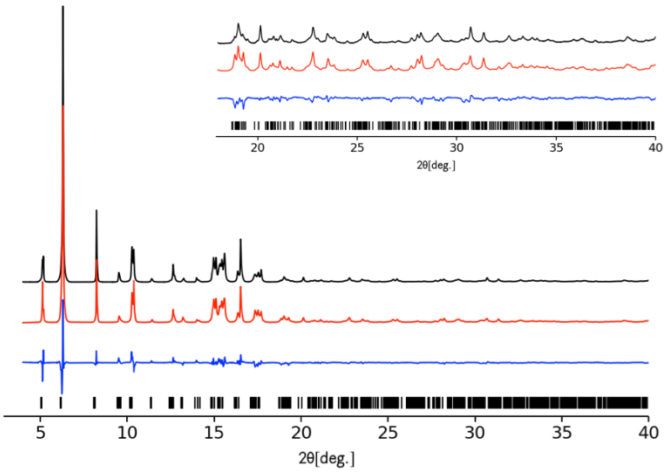

Figure 5: Observed (black), calculated (red) and difference (blue) profiles for the Rietveld refinement of IPC-4. The profiles in the inset have been scaled up by a factor of 6 to show more detail. Reflection positions are marked as vertical bar.

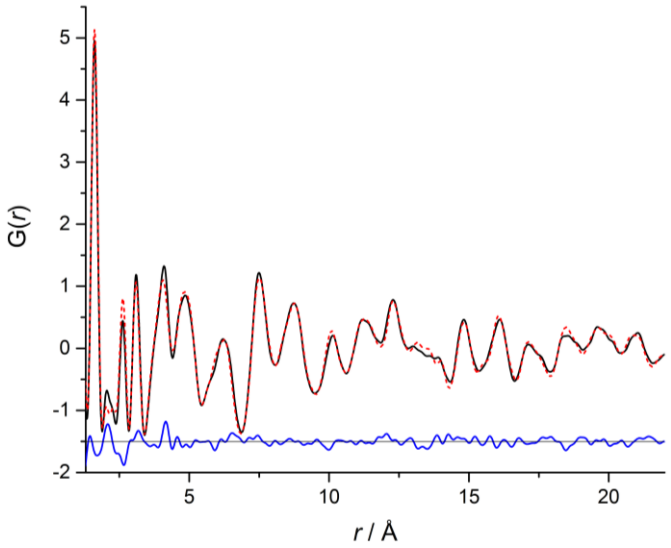

Figure 6: Refinement of the IPC-4 model against PDF data. Rw = 12.5 %. The black solid line is experimental data, the red dashed line is the calculated PDF from the model and the blue line is the difference between the two, offset by -1.5.

Table 5: PDF Refinement calculated structural parameters for IPC-1P.

	Average Si-O Bond length / Å	Average Si-O-Si Angle / °	Average O-Si-O Angle / °
PDF Refinement	1.61	154.5	109.5

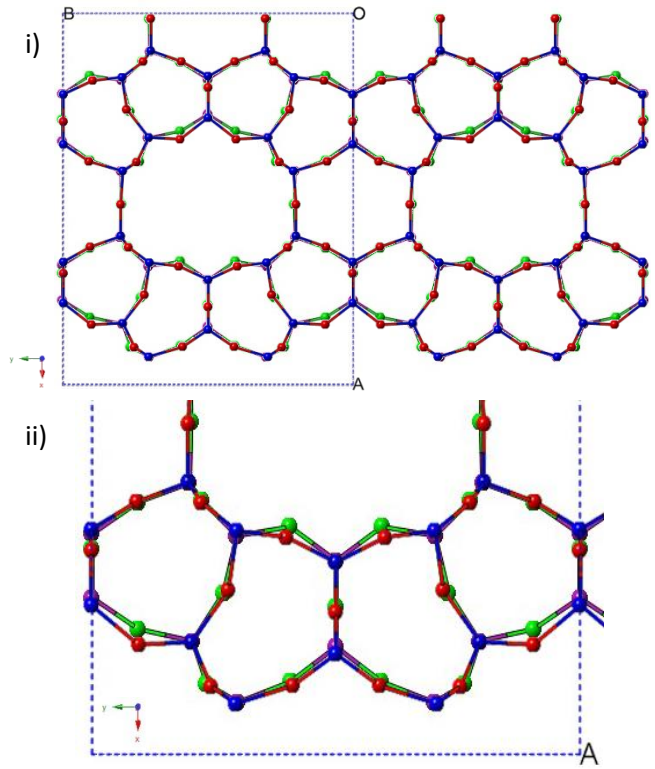

Figure 7: An overlap of IPC-4 (PCR) refinements by PDF (Si atoms in blue, O atoms in red) over Rietveld (Si atoms in purple, O atoms in green) showing the minimal difference between them. i) Shows two unit cells whilst ii) is a zoomed version to illustrate the finer differences. The unit cells have been rescaled to allow comparison and viewed down the c-axis.

O-Si-O angle is 109.1 °, the largest deviations occur around the interlayer connection, implying this region is the most disordered and strained - as is expected and observed with IPC-2.

Table 4 shows a comparison of unit cell parameters derived by different methods for IPC-4 (PCR). The results are consistent given that different samples were used for each refinement technique showing PDF refinement can be used accurately for zeolite refinements.

The results for IPC-2 and IPC-4 are noteworthy as bond and angle constraints can be used in Rietveld refinements, while PDFGui doesn't have such restraints and thus, the extremely good fits of Rw = 14.5 and 12.5% support the validity of the models and the technique when applied to complex zeolitic systems with many atoms.

The IPC-1P layers can orient themselves in four different orientations with respect to one another,[30] out of the low energy models calculated by DFT, the model that would result in the formation of IPC-4 by direct condensation was chosen and symmetrised using PLATON[31] into C 2/m to act as a starting model for the PDF refinement (computational details can be found in the Supplementary Information). The Rw of the resulting fit was 18% in the range of 1.38 – 10 Å, this smaller fit range was chosen to focus on the intralayer region of the pattern, in order to show that the layers do remain intact (Fig.8). Inspection of the calculated bond lengths and bond angles shows, despite a lack of restraints, very well behaved parameters. The mean T-O distance is 1.61 Å with a range from 1.54 – 1.67 Å and the mean tetrahedral bonding angle (O-T-O) is 109.5 °, with a range of 104.0 – 113.5 °.

While the fit accurately describes the primary units of the structure out to ~ 3.3 Å, the largest discrepancy occurs at the peak at 4.1 Å that relates to the second coordination spheres such as the pentasil secondary building units and other ring structures. Both IPC-2 and IPC-4 models accurately describe this peak. One possible explanation for this is that there are some interlayer connections already formed even in the intermediate IPC-1P structure. This is consistent with the observations of silica rearrangements that occur during the formation of IPC-6.[18] The model describes all other peaks well and this confirms that the layers do remain intact throughout hydrolysis. Therefore a viable structure for IPC-1P has been determined and is shown in Fig 9.

Table 6 compares the unit cells of all PDF calculated models, and by measuring their interlayer distance (the distance from the bottom row of T atoms, to the top row of T atoms of the layer below) then it is obvious that the IPC-1P interlayer separation (4.65 Å) is closer to that of IPC-2 (5.30 Å)

than IPC-4 (3.05 Å). The PDF refined distance between IPC-1P layers differs little from the DFT starting model, which describes a hydrogen-bonding network occurring between the exposed silanol groups of the layers. The favourable hydrogen bonding can only occur when the layers separate slightly and so must outweigh the energy gained through closer Van de Waals bonds from further layer collapse.

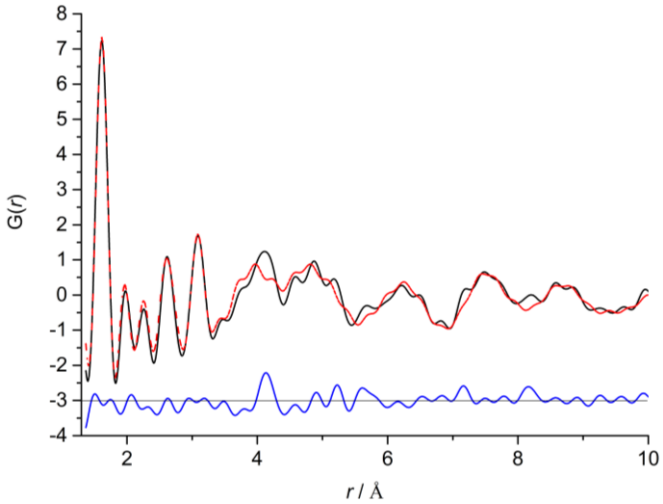

Figure 8: Refinement of the IPC-1P model against PDF data. Rw = 18.0 %. The black solid line is experimental data, the red dashed line is the calculated PDF from the model and the blue line is the difference between the two, offset by -3.

Table 6: A structural comparison of all structures calculated by PDF refinement. All structures were refined in the spacegroup C2/m.

Unit Cell	IPC-1P	DFT IPC-1P model	IPC-4	IPC-2
a / Å	25.03	24.58	20.07	23.78
b / Å	14.10	14.19	14.02	14.08
c / Å	12.24	12.54	12.44	12.40
α / °	90	90	90	90
β / °	119.1	119.1	115.7	109.1
γ / °	90	90	90	90
Interlayer Distance / Å	4.65	4.63	3.05	5.30

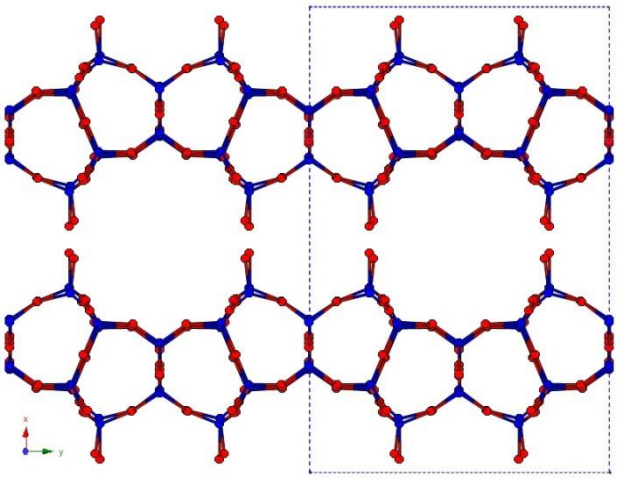

Figure 9: The PDF refinement of IPC-1P viewed down the c-axis. Si atoms in blue, O atoms in red.

Conclusions

The poorly crystalline structure of IPC-1P, the lamellar product of zeolite UTL hydrolysis, has been confirmed using pair distribution function analysis. This technique was first benchmarked against high-quality Rietveld analysis of structurally similar IPC-2 (OKO) and IPC-4 (PCR) structures and found to be reliable. Fitting used an initial model generated by density functional theory and gave R_w = 18% over a range of 1.3 - 10 Å. This proves the structure remains intact throughout the assembly, disassembly, organisation and reassembly process. Future work would include applying the PDF technique to the rest of the IPC-n series, data for this has already been collected and is currently being processed. An in-situ study of the assembly and disassembly process is also desired to monitor more accurately the structural changes occurring.

Acknowledgements

The Authors would like to thank: The EPSRC (grant EP/K025112/1) and the Czech Science Foundation grant no. P106/12/G015 (Centre of Excellence) for funding opportunities and beam lines I15 and I11 at the Diamond Light Source. Nicola Casati and Antonio Cervelino from the MS Powder beamline at the Swiss Light Source are acknowledged for their support in the data collection. A.B.P. acknowledges the support of the European Community under a Marie Curie Intra-European Fellowship for Career Development; and she is indebted to Lynne McCusker for showing her the secrets of Rietveld refinement in a playful, loving way.

Notes and references

1. J. Hermann, M. Trachta, P. Nachtigall and O. Bludský, *Catalysis Today*, 2014, **227**, 2-8.
2. M. Rutkowska, U. Díaz, A. E. Palomares and L. Chmielarz, *Applied Catalysis B: Environmental*, 2015, **168–169**, 531-539.
3. W. J. Roth, C. T. Kresge, J. C. Vartuli, M. E. Leonowicz, A. S. Fung and S. B. McCullen, *MCm-36: The first pillared molecular sieve with zeolite properties*, Elsevier Science Publ B V, Amsterdam, 1995.
4. J.-g. Jiang, L. Jia, B. Yang, H. Xu and P. Wu, *Chemistry of Materials*, 2013, **25**, 4710-4718.
5. P. Chlubná, W. J. Roth, H. F. Greer, W. Zhou, O. Shvets, A. Zukal, J. Čejka and R. E. Morris, *Chemistry of Materials*, 2013, **25**, 542-547.
6. H. Gies, U. Müller, B. Yilmaz, T. Tatsumi, B. Xie, F.-S. Xiao, X. Bao, W. Zhang and D. D. Vos, *Chemistry of Materials*, 2011, **23**, 2545-2554.
7. U. Diaz and A. Corma, *Dalton Transactions*, 2014, **43**, 10292-10316.
8. W. J. Roth, P. Nachtigall, R. E. Morris and J. Čejka, *Chem. Rev.*, 2014, **114**, 4807-4837.
9. W. J. Roth, O. V. Shvets, M. Shamzhy, P. Chlubná, M. Kubů, P. Nachtigall and J. Čejka, *Journal of the American Chemical Society*, 2011, **133**, 6130-6133.
10. W. J. Roth, P. Nachtigall, R. E. Morris, P. S. Wheatley, V. R. Seymour, S. E. Ashbrook, P. Chlubná, L. Grajciar, M. Položij, A. Zukal, O. Shvets and J. Čejka, *Nature Chemistry*, 2013, **5**, 628-633.
11. M. Shamzhy, M. Opanasenko, Y. Tian, K. Konysheva, O. Shvets, R. E. Morris and J. Čejka, *Chemistry of Materials*, 2014, **26**, 5789-5798.
12. P. Chlubná-Eliášová, Y. Tian, A. B. Pinar, M. Kubů, J. Čejka and R. E. Morris, *Angewandte Chemie International Edition*, 2014, **53**, 7048-7052.
13. R. E. Morris and J. Cejka, *Nat Chem*, 2015, **7**, 381-388.
14. P. Eliasova, M. Opanasenko, P. S. Wheatley, M. Shamzhy, M. Mazur, P. Nachtigall, W. J. Roth, R. E. Morris and J. Cejka, *Chemical Society Reviews*, 2015, **44**, 7177-7206.
15. M. Mazur, P. S. Wheatley, M. Navarro, W. J. Roth, M. Položij, A. Mayoral, P. Eliášová, P. Nachtigall, J. Čejka and R. E. Morris, *Nat Chem*, 2016, **8**, 58-62.
16. M. Mazur, M. Kubů, P. S. Wheatley and P. Eliášová, *Catalysis Today*, 2015, **243**, 23-31.
17. P. S. Wheatley, P. Chlubná-Eliášová, H. Greer, W. Zhou, V. R. Seymour, D. M. Dawson, S. E. Ashbrook, A. B. Pinar, L. B. McCusker, M. Opanasenko, J. Čejka and R. E. Morris, *Angewandte Chemie International Edition*, 2014, **53**, 13210-13214.
18. M. Mazur, P. Chlubná-Eliášová, W. J. Roth and J. Čejka, *Catalysis Today*, 2014, **227**, 37-44.
19. M. M. Martínez-Iñesta and R. F. Lobo, *The Journal of Physical Chemistry B*, 2005, **109**, 9389-9396.
20. M. M. Martínez-Iñesta, I. Peral, T. Proffen and R. F. Lobo, *Microporous and Mesoporous Materials*, 2005, **77**, 55-66.
21. P. K. Allan, K. W. Chapman, P. J. Chupas, J. A. Hriljac, C. L. Renouf, T. C. A. Lucas and R. E. Morris, *Chemical Science*, 2012, **3**, 2559-2564.
22. X. Hua, R. Robert, L. S. Du, K. M. Wiaderek, M. Leskes, K. W. Chapman, P. J. Chupas and C. P. Grey, *J. Phys. Chem. C*, 2014, **118**, 15169-15184.
23. K. W. Chapman, *MRS Bull.*, 2016, **41**, 231-238.
24. B. Key, M. Morcrette, J.-M. Tarascon and C. P. Grey, *Journal of the American Chemical Society*, 2011, **133**, 503-512.
25. E. Verheyen, L. Joos, K. Van Havenbergh, E. Breynaert, N. Kasian, E. Gobechiya, K. Houthoofd, C. Martineau, M. Hinterstein, F. Taulelle, V. Van Speybroeck, M. Waroquier, S. Bals, G. Van Tendeloo, C. E. A. Kirschhock and J. A. Martens, *Nat Mater*, 2012, **11**, 1059-1064.
26. L. A. Villaescusa, P. Lightfoot, S. J. Teat and R. E. Morris, *Journal of the American Chemical Society*, 2001, **123**, 5453-5459.
27. I. Bull, P. Lightfoot, L. A. Villaescusa, L. M. Bull, R. K. B. Gover, J. S. O. Evans and R. E. Morris, *Journal of the American Chemical Society*, 2003, **125**, 4342-4349.
28. A. Coelho, *Journal of Applied Crystallography*, 2003, **36**, 86-95.
29. L. Grajciar, O. Bludský, W. J. Roth and P. Nachtigall, *Catalysis Today*, 2013, **204**, 15-21.
30. A. Spek, *Acta Crystallographica Section D*, 2009, **65**, 148-155.